41st International Conference on Environmental Systems
17 - 21 July 2011, Portland, Oregon

AIAA 2011-5112

Spacecraft Cabin Acoustic Modeling and Validation with Mockups

S. R. Chu[1]
Lockheed Martin, 1300 Hercules, M/C: C46 P.O. Box 58487, Houston, TX 77258

and

C. S. Allen[2]
NASA Johnson Space Center, Mail Code SF22, 2101 NASA Road 1, Houston, TX 77058

This paper describes the implementation of acoustic modeling for design purposes by incrementally increasing model fidelity and validating the accuracy of the model while predicting the noise of sources under various conditions. An International Space Station (ISS) US Lab mockup and an Orion Crew Module (CM) acoustic mockup were used for modeling validation. The latest configuration of the CM acoustic mockup and corresponding model include a ventilation system mockup and an ECLSS (Environmental Control and Life Support System) wall, associated closeout panels, and the gaps between ECLSS wall and mockup wall. The effects of sealing the gaps and applying sound absorptive treatment to the ECLSS wall were thoroughly modeled and validated.

Nomenclature

T_{60}	=	reverberation time of an acoustic cavity
$\overline{T}_{60}$	=	average reverberation time of an acoustic cavity
$\overline{\alpha}$	=	average absorption coefficient of an acoustic cavity
$\overline{\alpha}_w$	=	average absorption coefficient of an acoustic cavity by layup model of Noise Control Treatment
V	=	volume of an acoustic cavity
S	=	internal surface area of an acoustic cavity
c	=	speed of sound
Fs	=	Schroder frequency
m	=	air attenuation in dB per 1000 m
SPL	=	Sound Pressure Level
SEA	=	Statistical Energy Analysis
CM	=	Crew Module
RSS	=	Reference Sound Source
ECLSS	=	Environmental Control and Life Support System
ISS	=	International Space Station
MDF	=	Medium-Density Fiberboard
NCT	=	Noise Control Treatment
FA	=	Field Angle
SIF	=	Semi-Infinite Fluid
TL	=	Transmission Loss
VTL	=	Virtual Transmission Loss
DLF	=	Damping Loss Factor
IL	=	Insertion Loss
PIM	=	Power Injection Method

[1] Staff Mechanical Engineer, Acoustics and Noise Control Lab
[2] Deputy Chief, Environmental Factors Branch, Habitability & Environmental Division, Space Life Sciences Directorate

I. Introduction

Acoustic modeling can be used to identify key noise sources, determine/analyze sub-allocated requirements, keep track of the accumulation of minor noise sources, and to predict vehicle noise levels at various stages in vehicle development, first with estimates of noise sources, later with experimental data. This paper describes the implementation of acoustic modeling for design purposes by incrementally increasing model fidelity and validating the accuracy of the model in predicting the mockup interior SPL under various noise sources. During 2007, a simple-geometry SEA model was built using VA One commercial modeling software from ESI Group and validated using a physical mockup and acoustic measurements. The dimensions of the rectangular-shaped mockup interior was similar to the interior of the ISS US Lab as shown in Figs. 1 and 2. A process for modeling the effects of absorptive wall treatments and the resulting reverberation environment were developed. During 2008, a model with a more complex and representative geometry of the Orion CM interior was built again using VA One, and noise predictions based on input noise sources were made. A corresponding physical mockup was also built. Measurements were made inside this mockup, and comparisons were made with the model and showed excellent agreement. During 2009, the fidelity of the Orion CM mockup and corresponding model were increased incrementally by including a simple ventilation system mockup. The airborne noise contribution of the fans was measured using a sound intensity technique, since the sound power levels were not known beforehand. This is opposed to earlier studies where RSSs with known sound power levels were used. Comparisons of the modeling result with the measurements in the mockup showed excellent results. During 2010, the fidelity of the CM mockup and the model were further increased by including an ECLSS wall, associated closeout panels, and the gaps between ECLSS wall and mockup wall. The effect of sealing the gaps and adding sound absorptive treatment to ECLSS wall were also modeled and validated. Note that the ECLSS wall is a group of closeout panels that separate the ECLSS equipments (including fans, pumps, etc.) from the crew habitable volume, i.e., the cabin.

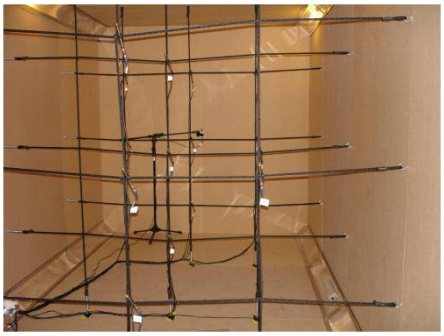

Figure 1. ISS US Lab Acoustic Mockup interior.

Figure 2. ISS US Lab Acoustic Mockup exterior.

II. Modeling/Validation of ISS US Lab Mockup

During 2007, a SEA model of the ISS US Lab mockup, with walls made of one layer of MDF and one layer of plywood, was constructed. These dense wall materials were used here for better trapping sound inside the mockup to simulate the on-orbit situation. The activity of this phase was focused on understanding of how a SEA model represents airborne noise sources with known sound power levels in a rectangular-shaped enclosure. The mockup is not full scale in the longitudinal axis, i.e., 2/3 of the length of the US Lab. Also, no attempt was made to replicate the ISS acoustic environment, i.e., no racks, no ventilation systems, etc. Single and two RSSs were used to excite the mockup. RSS is an electric-motor-driven impeller system, which produces a relatively flat, significant, and repeatable sound power spectrum over a wide frequency range. The sound power levels of our RSSs were calibrated annually, and were the inputs to the model. Three mockup interior reverberant environments were modeled : 1) bare interior wall, 2) all the interior wall surfaces completely covered by one layer of the sound absorptive material Thinsulate^{TM}, and 3) all the interior wall surfaces completely covered by two layers of Thinsulate. The selection of Thinsulate was just to validate various methods of modeling sound absorptive treatment using VA One. Two methods of modeling mockup were developed. The model was validated based on the accuracy of SPL predictions over 1/3-octave bands by comparing with the average of simultaneously measured SPLs at seventeen locations inside the mockup.

A. Acoustic Model of ISS US Lab Mockup

The first method of modeling the mockup interior absorption was by measuring the T_{60} of the interior. T_{60} is the time for the SPL of a cavity to decay 60 dB from its initial level without any sound source in the cavity. A fixed set of 7 microphones in the mockup interior was used for the measurement. According to ISO 3382 in Ref. 1, microphone positions should be at least half wavelength apart for the lowest frequency, and any microphone position should be at least quarter wavelength from nearest reflecting surface. It was determined that 172 Hz is the lowest frequency for our setup that the above criterion is satisfied. A total of eight tests were performed with one impulse source such as a party "popper" placed at one of the 8 corners of the mockup during each test. This is the impulse method of measuring T_{60}.Brüel Kjær (B&K) Pulse room acoustic software was used to determine the decay curves for the microphone signals. The software computed T_{30} or T_{20} from the decay curve, depending on decaying range being at least 35 or 25 dB, and extrapolated the result to obtain T_{60}. T_{60}'s of the microphones were averaged to obtain the T_{60} for each "popper" location. The resulting T_{60}'s were further averaged to obtain the average $\overline{T}_{60}$ of the mockup interior. The mockup cavity average absorption was then calculated from the average $\overline{T}_{60}$ based on the following Sabine equation.

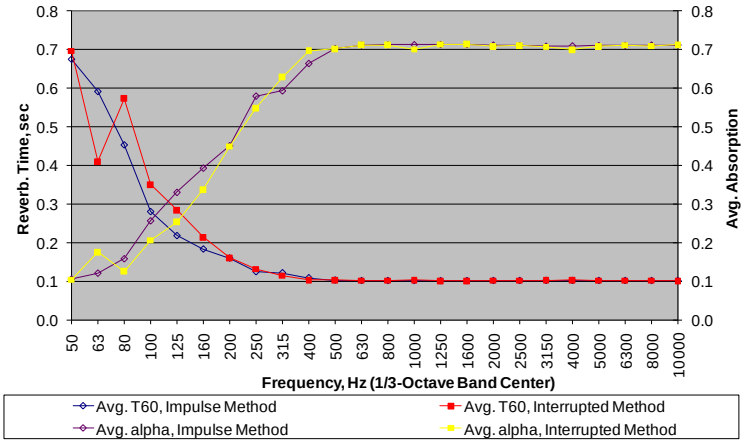

Figure 3. Reverberation time and average absorption, impulse vs. interrupted method, US Lab Acoustic Mockup covered by two layers of Thinsulate.

$$\bar{\alpha} = \frac{55.25V}{Sc\overline{T}_{60}} \tag{1}$$

An alternative method of measuring T_{60}, the interrupted method, was also used to measure the T_{60} of the interior. A loudspeaker, driven by amplified pink noise, was used to excite the mockup interior cavity for 5.2 sec, then the signal was turned off abruptly, and SPLs of all the microphones were monitored for calculating the decay curves. Both T_{60} measurement methods were used for mockup interior wall covered by 1 layer and 2 layers of Thinsulate. Figure 3 indicates that the resulting T_{60} measurements from both methods were consistent. The $\bar{\alpha}$ was then applied to the cavity of the mockup model as the absorption coefficient.

The second method of modeling the mockup interior absorption was done by performing impedance tube testing on one- and two-layered Thinsulate samples per the standards in ISO 10534-2 or ASTM E1050.[2,3] The narrowband frequencies, the sound absorption coefficients, the complex

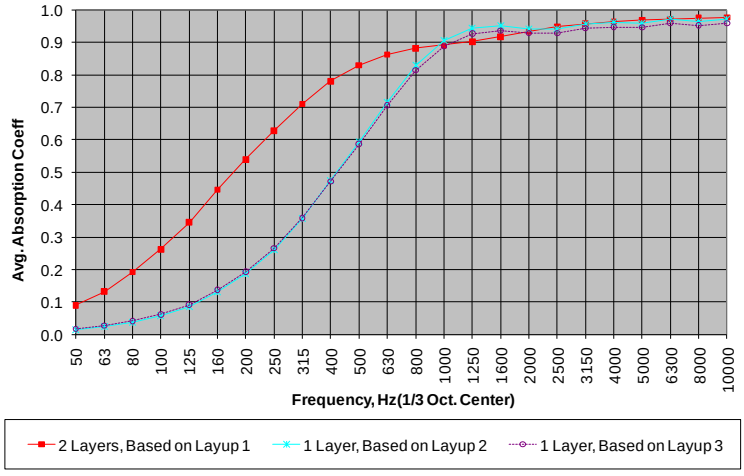

Figure 4. Cavity Absorption Comparison: 2 layers vs. 1 layer of Thinsulate, Layup Model vs. Sabine Equation (with Measured T_{60}). Layup 1: Thinsulate + 1mm Gap + Thinsulate + 2mm Gap, Max FA 78 deg; Layup 2: Thinsulate + Various Gap, Max FA 78 deg; Layup 3: AU6020-6 + Various Gap, Max FA 89 deg.

reflection coefficients, and the complex normalized surface impedance of the measurements were entered into the software ESI FOAM-X, which performed curve fitting on measured absorption and identifies the following five fibrous material properties:

- Static airflow resistivity, which expresses the frictional effect on airflow through pores.
- Open porosity, which defines the fraction of the volume that is occupied by air in the interconnected porous network.
- Viscous characteristic length, which is an average macroscopic dimension of cells related to viscous losses. It may been seen as an average radius of smaller pores of a porous aggregate.
- Thermal characteristic length, which is an average macroscopic dimension of cells related to thermal losses. It may been seen as an average radius of larger pores of a porous aggregate.
- Geometrical tortuosity, which is a geometrical measurement of the actual path followed by an acoustic wave from a direct path.

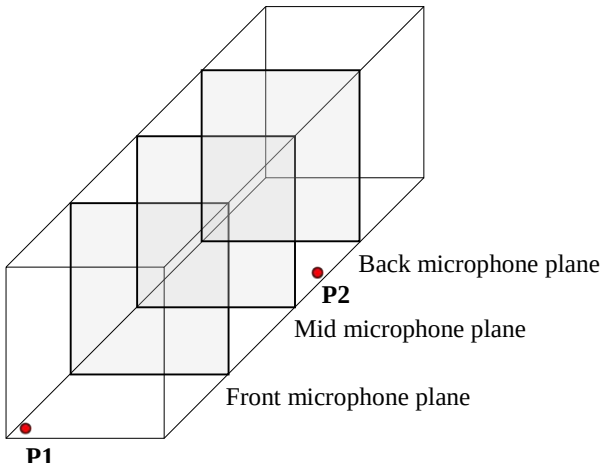

Figure 5. Locations of the single RSS for SPL measurements in bare US Lab Mockup.

The parameter identification performed by FOAM-X was based on an extension of the Biot theory of porous media to elastic porous acoustic materials[8], which includes an elastic porous (foam) model, a limp porous (fiber) model, and a rigid (fiber) model. The Foam Module of the VA One software also uses similar models for absorption prediction. Both limp porous model and rigid porous models were tested, and the rigid porous model was used due to better curve fitting results. The identified parameters were transferred to the VA One Foam Module to build single- and two-layered NCT layup models. A thin air gap layer of 1-2 mm was specified between the mockup wall and neighboring fiber layer as well as between two fiber layers to model that a Thinsulate layer was not bonded to the wall and that the two Thinsulate layers were not continuous. Also, if the measured thickness of a Thinsulate treatment was more than 2 mm thicker than the official thickness published by the manufacture, 3M, an air gap of the difference in thickness was specified between the treatment and the wall. The layup model traces the incident energy and the energy dissipated by absorption. Incident sound intensity is assumed to be uniformly distributed over all incident angles above 90 deg minus a maximum field angle. The default maximum FA was set at 78 deg.

Figure 4 shows that two layers of Thinsulate provide more absorption compared to one layer of Thinsulate only for low and mid frequencies, i.e., below 1,000 Hz.

B. Model Validation for ISS US Lab Mockup

The ISS US Lab mockup model was validated based on SPL prediction accuracy over 1/3-octave bands by comparing with the average of simultaneously measured SPLs at seventeen locations. RSS sound power from accredited calibration service was the input to the model. In the case of excitation by 2 RSSs, the input sound power level is the logarithmic sum of individual RSS sound power levels. For the bare US Lab mockup, Fig. 6 shows that the location of RSS had virtually no effect on the average of measured SPLs. Figure 5 depicts the locations the single RSS for the SPL measurements. The prediction of the model matches very well with the average of measured SPLs for frequency bands over 315 Hz. The spread of measured SPLs, due to excitation by a single RSS at location P2, is well within +/- 3 dB of the prediction for frequencies over 315 Hz as shown in Fig. 7. This indicates that a diffuse sound field was formed inside the mockup, which is suitable for SEA analysis. Wide swings of SPL at low frequencies were due to the domination of standing waves and not enough acoustic modes to support a diffuse field for accurate SEA prediction. The lowest frequency at which the modal density is sufficient to support a diffuse field can be estimated, for a three-mode overlap, by the Schroder frequency, which can be calculated as

$$F_s = \sqrt{\frac{c^3 \overline{T}_{60}}{4V \ln 10}} \tag{2}$$

Fs was found to be 591 Hz using T_{60} at 630 Hz. Furthermore, the mockup wall has low transmission loss at low frequencies, and this contributes to the apparent overestimation in SPL.

After the bare mockup model was validated, the models of the mockup with interior surfaces completely covered by one layer and then two layers of Thinsulate were validated next. Both configurations created highly absorptive environments inside the mockup, particularly in mid and high frequencies as shown in Fig. 4. This yielded a sound field less diffuse as compared to inside the bare mockup. The spread of measured SPLs was outside of the +/- 3 dB desired accuracy margin around the SEA prediction. This wider spread shouldn't be interpreted as insufficient modal overlap as the Schroder frequency decreases compared to bare mockup. Actually, measured SPL was found to be decaying from the source along the longitudinal axis of the mockup if a single RSS was placed at the front corner of the mockup. It is evident from Fig. 8 that the average SPL was decaying from the front to the back microphone plane. As opposed to the bare mockup, the location(s) of RSS(s) had some influence on SPL distribution and hence the prediction accuracy of a single-cavity mockup model. It was found that, as long as no RSS was placed at or near front (rear) corners, or against the front (rear) wall, the prediction of the single-cavity model matches well with the average of measured SPLs as shown in Fig. 10. Figure 10 also shows that the match is particularly good if the RSS is placed near the center of the mockup as indicated by location P7. On the other hand, if the RSS is placed at or near the front corners, the prediction of the model is at least 3 dB over the average of measured SPLs as shown in Fig. 11. Figure 12 shows that the over prediction is even greater than that shown in Fig. 11 when the cavity absorption is predicted from measured T_{60}. Note that Fig. 9 shows the locations of the single RSS used in the SPL comparisons as depicted in Figs. 10 thru 12.

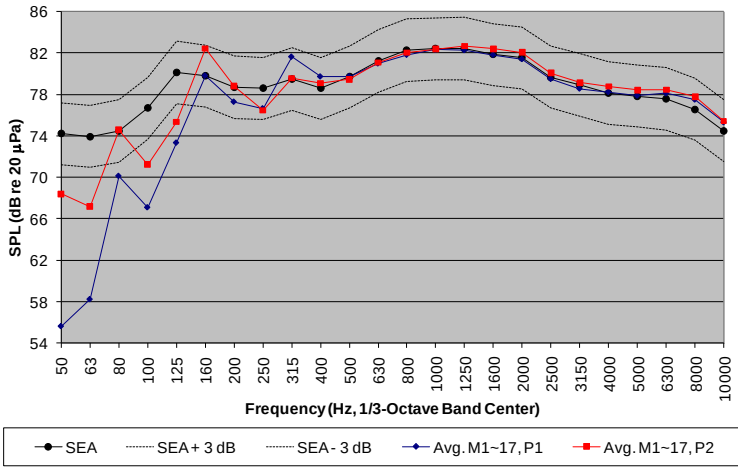

Figure 6. SEA prediction vs. average of measured SPLs in bare US Lab Mockup, single RSS excitation at locations P1 and P2, absorption from measured T_{60}.

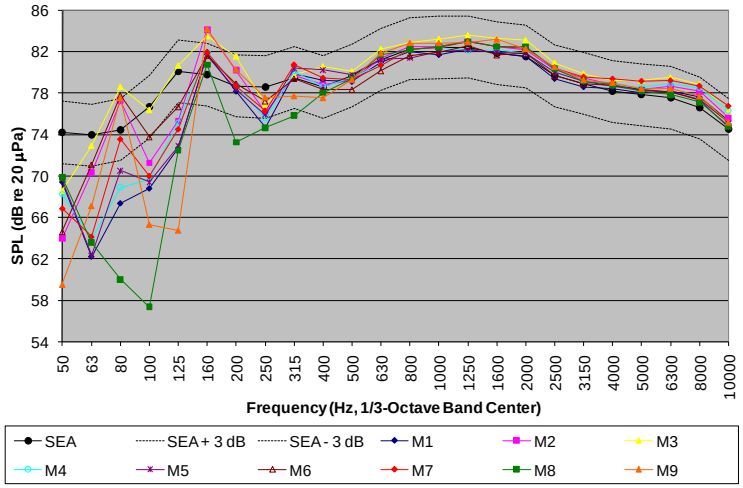

Figure 7. SEA prediction vs. measured SPL distribution in bare US Lab Mockup, single RSS excitation at location P2, absorption from measured T_{60}.

It is clear that the disagreement shown in Figs 11 and 12 is caused by the fact that with such high absorption, one of the underlying assumptions of SEA, that the acoustic field is diffuse, is not upheld for such large mockup cavity. The original model was then subdivided into three cavities as shown in Fig. 13. The smallest cavity at the front lower left corner is the source cavity, which is around the single RSS. The next largest cavity is the back cavity, which contains the back microphone plane. The largest cavity contains both the front and mid microphone planes, but excludes the source cavity. Figure 14 indicates that the SPLs of the largest and next largest cavities match very well with the average SPLs of the front/mid microphone planes, and the back microphone plane, respectively, for frequencies above 500 Hz. This demonstrates that cavity subdivision can compensate somewhat for the effect of high absorption on SPL distribution in a large cavity. But it must proceed with caution that each cavity has sufficient number of modes to support a diffuse acoustic field. "Modes in Band" analysis was performed, and all three cavities

were found to have sufficient number of modes. The general rule of thumb is that a cavity should have at least 3 modes in a frequency band to sustain a diffuse field in the band. The source cavity had the least number of modes in band and satisfied the above criterion for frequency bands above 500 Hz. The remaining two larger cavities satisfied the criterion in much lower frequencies. This part of the study was undertaken to test the limits of SEA predictive capability. Fortunately, this level of absorption is much higher than what exists in actual spaceflight vehicles, as the following discussion will reveal.

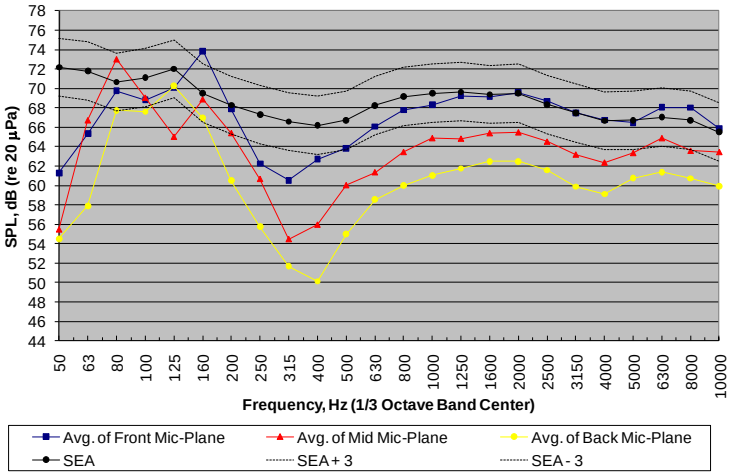

Figure 8. SEA prediction (single-cavity model) vs. average SPLs for front/mid/back microphone planes in US Lab Mockup covered by 2 layers of Thinsulate, single RSS excitation at the front lower left corner, absorption from layup model.

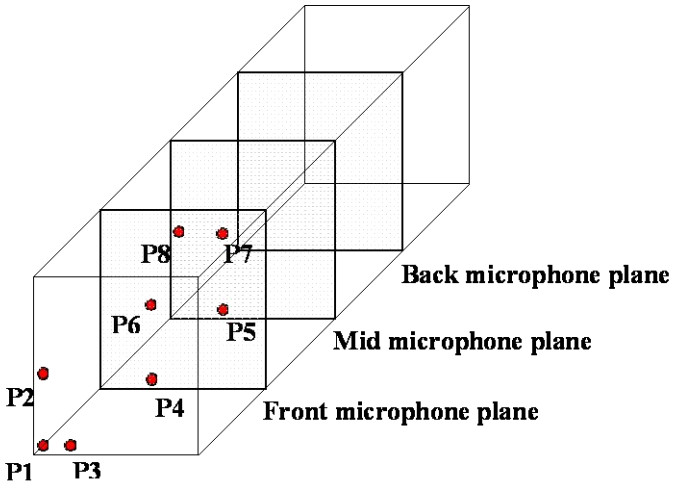

Figure 9. Locations of the single RSS for SPL Measurements in US Lab Mockup covered by 2 layers of Thinsulate.

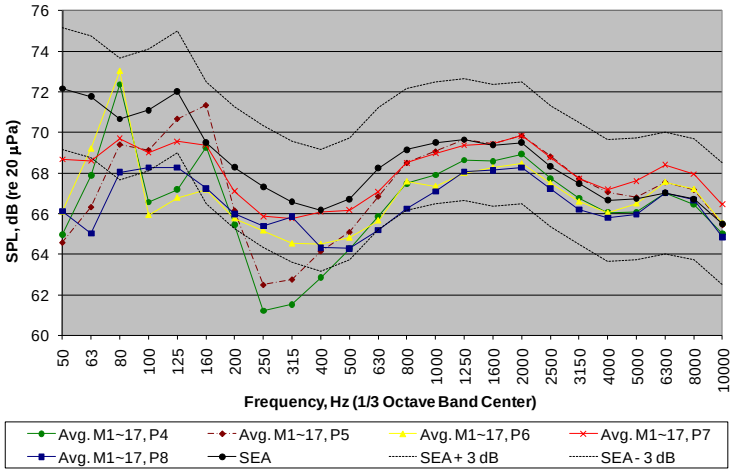

Figure 10. SEA prediction vs. average of measured SPLs in US Lab Mockup covered by 2 layers of Thinsulate, single RSS excitation at various locations away from the front corners, absorption from layup model.

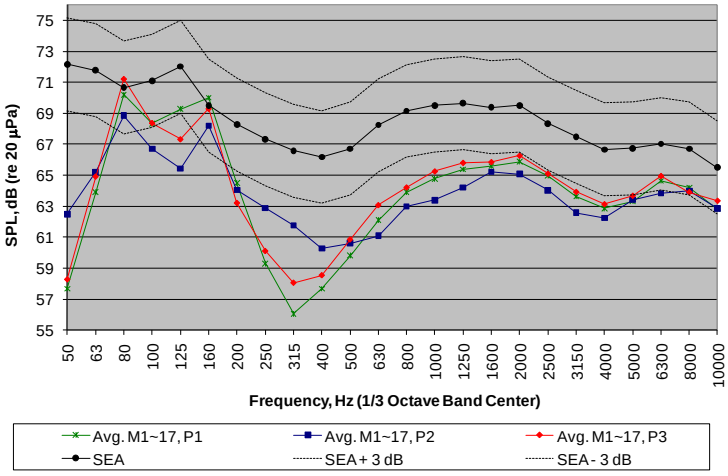

Figure 11. SEA prediction vs. average of measured SPLs in US Lab Mockup covered by 2 layers of Thinsulate, single RSS excitation at or near front corner, absorption from layup model.

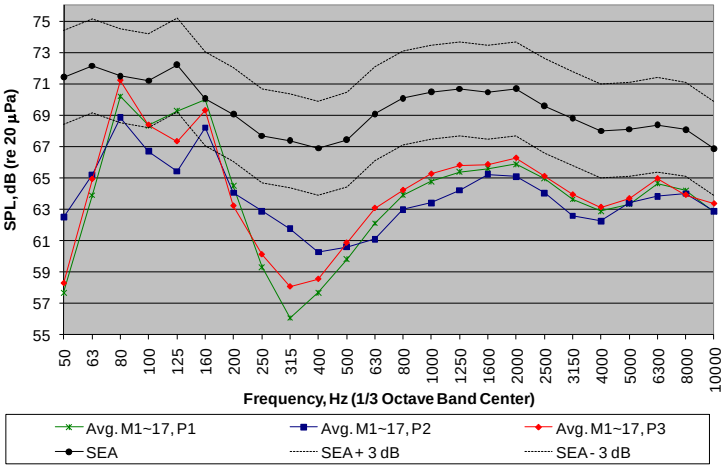

Figure 12. SEA prediction vs. average of measured SPLs in US Lab Mockup covered by 2 layers of Thinsulate, single RSS excitation at or near front corners, absorption from measured T_{60}.

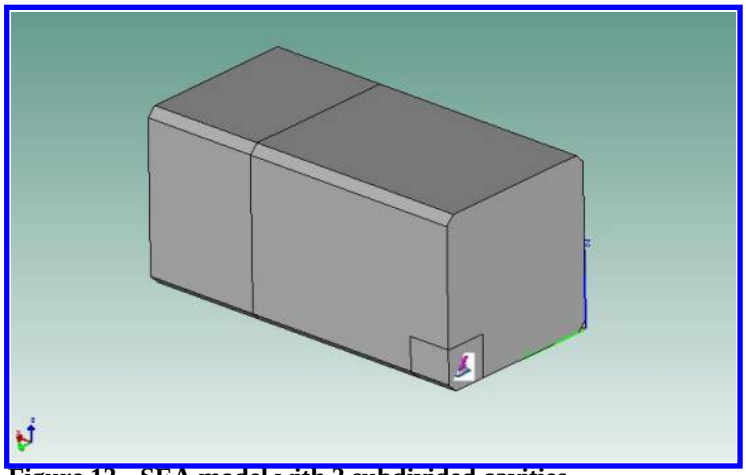

Figure 13. SEA model with 3 subdivided cavities.

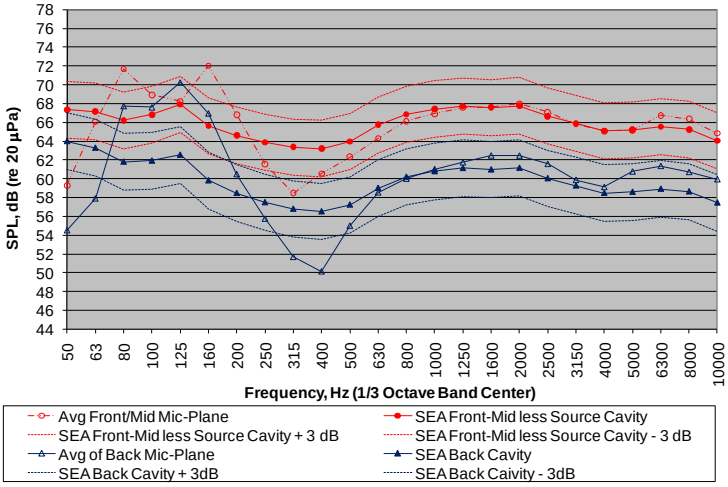

Figure 14. SEA prediction (with subdivided cavities) vs. averages of front-mid/back microphone plane SPLs in US Lab Mockup covered by 2 layers of Thinsulate, single RSS excitation at front lower left corner, absorption from layup model.

III. Modeling/Validation of Orion CM Mockup

During 2008, the Orion CM acoustic mockup, with more complex geometrical shape than the ISS US Lab mockup, was constructed as shown in Fig. 15. The initial configuration of the CM mockup contained a 12-faced enclosure made of two-layered MDF walls, which are more massive than the wall of the US Lab mockup. The volume of the mockup interior matches that of the Orion pressure vessel, with the shape and the surface area very close to the vessel. The activity during this period was still focused on validating a SEA model with more complex shape in representing airborne noise sources with known sound power levels, such as single and two RSSs. Only the bare mockup was studied.

Figure 15. Orion CM Acoustic Mockup exterior, wall made of 2 MDF sheets, 1 inch total thickness.

During 2009, the focus was to validate the CM model in representing a single airborne noise source with unknown sound power level. Two ventilation system mockups, a small fan (Sanyo Denki SanAce120L 9GL 1224J102) in a 5 inch square MDF duct and a large fan (Comair Rotron JQ24B8) in a 6 inch diameter PVC pipe, were used for the validation. Both fans have 7 blades. The sound power levels of these fans were available in our quiet fan database with flow rate up to 231 cfm for the large fan and 176 cfm for the small fan. The flow rates of the fans could not be determined accurately during the time of the validation. Therefore, the sound power levels were estimated based on sound intensity measurement and used in the mockup model for SPL prediction. The interior wall of the mockup was partially covered by two layers of Thinsulate, which reduced mockup interior reverberation levels similar to ISS US Lab for speech bands, i.e., 500, 1k, 2k, and 4kHz. The mockup in this configuration has been used for developing a new requirement for Orion post-landing speech interference limit.

During 2010, the fidelity of the mockup and the model were further increased by including an ECLSS wall, associated closeout panels, and the gaps between the ECLSS wall and the mockup wall simulating the construction of the Orion vehicle. The ECLSS wall consists of 7 sandwich panels. Each panel is made of Aluminum honeycomb core and Aluminum skin. The sizes, i.e. the widths, of the gaps vary from 1 inch to 3 inches. The locations of the gaps are shown in Figs. 32 and 37. . Modeling and validations were performed for 4 configurations:

- Bare mockup and bare ECLSS wall with open gaps.

- Bare mockup and bare ECLSS wall with sealed gaps.
- Bare mockup and ECLSS wall with sealed gaps, one layer of Thinsulate attached to the cabin side of the ECLSS wall on all 7 panels.
- Bare mockup and ECLSS wall with sealed gaps, one layer of Thinsulate attached to the cabin side of the ECLSS wall on 4 panels, and to the ECLSS bay side of the ECLSS wall on the remaining panels.

For the above 4 configurations, both RSS and ventilation mockup were placed separately inside the ECLSS bay. It will be shown in the following by both modeling and measurements that deploying part of available absorption material inside the source cavity is more effective in reducing the SPL in the cabin than deploying all the absorption material in the receiver cavity.

A. Model of Bare CM Mockup, No ECLSS Wall, Excitation by RSS(s)

Unlike the model of the US Lab mockup, the mockup wall of the CM mockup model was not treated as acoustically stiff. Mechanical properties of MDF and Schedule 80 PVC were used to model the wall, the deck, and docking tunnel. SEA SIFs were used to model sound radiation from the exterior surfaces of the mockup to a free field. The sound, reflected from the wall of the room where the mockup was located and reentered the mockup again, was not modeled due to significant TL of MDF.

The cavity absorption of the mockup was calculated from the average reverberation time $\overline{T}_{60}$ of the mockup interior based on the Sabine equation. The $\overline{T}_{60}$ was obtained by averaging the T_{60}'s from four tests, which were performed using the interrupted method. Each test was conducted with different locations of single speaker and five microphones.

Figure 16. Bare Orion CM Acoustic Mockup interior and microphones.

B. Model Validation for Bare CM Mockup, No ECLSS Wall, Excitation by RSS(s)

The mockup model was validated based on SPL prediction accuracy over 1/3-octave bands by comparing with the average of simultaneously measured SPLs at ten microphones located at two planes with each plane having five microphones as depicted in Fig. 16. The prediction of the model matches very well with the average of measured SPLs for excitation by single RSS and two RSSs. Figure 17 shows that measured SPLs are also very close to the model prediction for frequency bands over 500 Hz. The estimated Fs is 610 Hz based on T_{60} at 630 Hz. However, one exception was discovered when a RSS was placed at the center of the mockup floor. Figure 18 shows that the model prediction deviates more from the average of measured SPLs as compared to Fig. 17. Figure 18 further shows that SPLs at the axis of the symmetry of the mockup, i.e., microphones 2 and 7, exceed the prediction significantly for a wide frequency range. The difference was thought to be due to the fact that the mockup wall tends to focus its first reflections on the axis of symmetry, if the source is located at the center. This is illustrated in Figs. 19 and 20. To validate the hypothesis, a three-sided box was constructed to redirect the emissions of the RSS to only part of the mockup wall as shown in Fig. 21. Figure 22 indicates significant reduction of SPLs at microphones 2 and 7. The model prediction has much better agreement with the measurement under this situation.

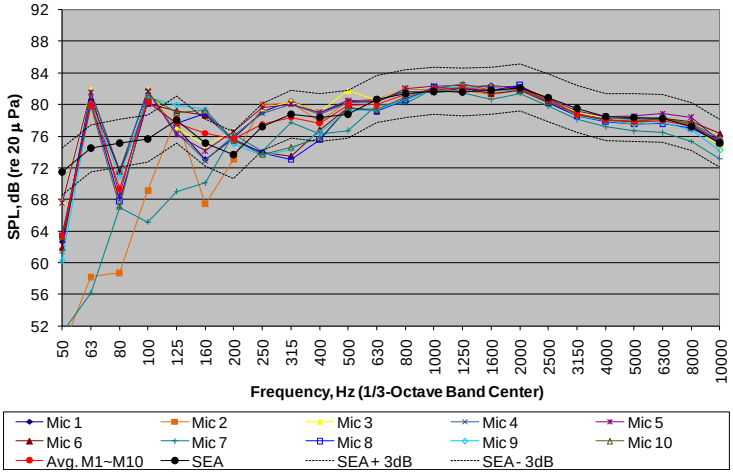

Figure 17. SEA prediction vs. measured SPL distribution in bare Orion CM Mockup, excitation by a single RSS not at the center of mockup floor, i.e., against the mockup wall.

C. Model of CM Mockup with Thinsulate, No ECLSS Wall, Excitation by Fan Source

The mockup interior wall was covered **partially** by two layers of Thinsulate. The covered wall formed three groups of contiguous surfaces and alternate with three groups of wall surfaces not covered by Thinsulate as shown in Fig. 23, 28, and 29. The cavity absorption of the mockup was modeled similarly as before:

- Sabine equation using measured $\overline{T}_{60}$. The interrupted method was used with a newly purchased B&K dodecahedron speaker, which is also shown in Fig. 23.
- Two-layered Thinsulate layup model as developed before for the ISS mockup. The percentage of coverage was specified in the mockup model.
- Two-layered Thinsulate layup model with correction for absorption by air. Let $\overline{\alpha}_w$ be the cavity absorption due to the layup model, then the overall cavity absorption is[4]

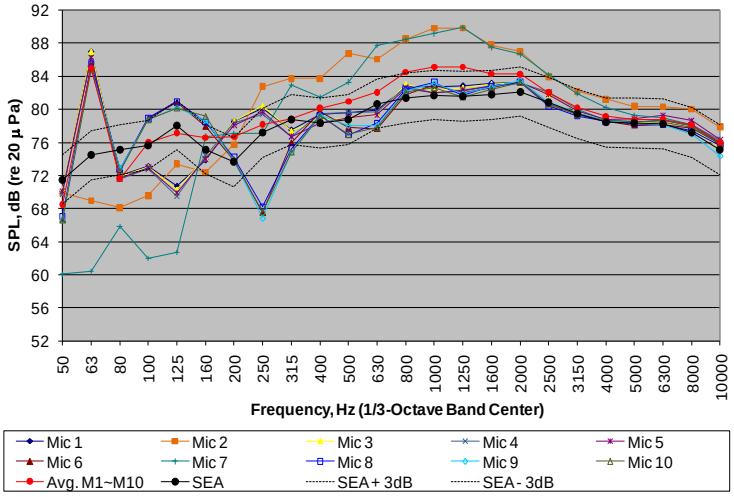

Figure 18. SEA prediction vs. measured SPL distribution in bare Orion CM Mockup, excitation by single RSS at the center.

$$\overline{\alpha} = \overline{\alpha}_w + 9.21\times10^{-4} mV/S \tag{3}$$

where m is air attenuation in dB/1000 m. m for 20ºC and 50% relative humidity was used. Air attenuation is proportional to the volume-to-surface-area ratio of the mockup cavity. It has been shown that the ratio is related to the mean free path for sound wave traveled in an arbitrarily shaped cavity between reflections[4].

The mockup was subject to one fan excitation, i.e., the large fan or the small fan. The unknown sound powers of these fan sources were estimated from sound intensity measurement using a B&K 3599 sound intensity probe, B&K 4197 phase matched 0.5" microphones, and B&K Pulse intensity mapping software. The estimated sound power was used as the input to the mockup model. A grid system of rectangular box shape was built for the sound intensity measurements. The grid system enclosed the source to be measured with five surfaces, i.e., front, right, back, left, and top. Sound intensity at the center of each segment of the grid system was measured and time averaged for 15 sec. Sound intensity at the bottom surface could not be measured. In order to estimate sound power, the source was placed on highly reflective surface so that it could reflect most of the incident sound energy back to the measured surfaces.

The sound intensity of a RSS was measured first to validate the procedure of estimating sound power from sound intensity measurement. A measurement grid of cubic box shape with 3x3 segments on each enclosing surface was used. Deviation of estimated sound power from calibrated sound power was found to be small (< 1 dB) for octave bands from 125 Hz to 4 kHz using only the 12 mm microphone spacer. The estimated sound power was 4.1 dB below the calibrated sound power for the 8 kHz octave band. The accuracy can be improved by using either 0.25" microphones with 8.5 mm spacer or

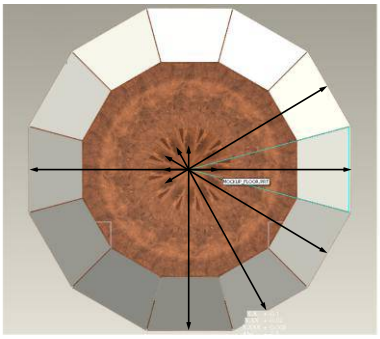

Figure 19. Focusing of mockup walls first reflection, top view.

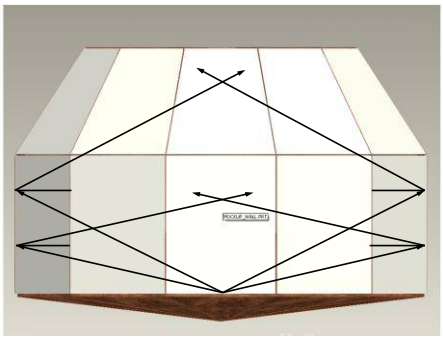

Figure 20. Focusing of mockup walls first reflection, side view.

microphone response equalization. The equalization is not just for the response for a single microphone, but for a pair of microphones in a face-to-face configuration. According to the B&K data sheet, the intensity measurement can be extended from 5 kHz to 10 kHz using just the 12 mm spacer and software implemented microphone response equalization, which was not available in our Pulse system. Therefore, 4.1 dB was added to the estimated sound powers of the small fan and large fan. Deviation from calibrated sound power at the 63 Hz octave band was also greater than 1 dB, which can be improved by using a wider spacer such as the 50 mm spacer. However, the measurement accuracy is further limited by phase mismatch of the entire measurement chain and SEA prediction is not very accurate at low frequency end. Therefore, the estimated sound power at the 63 Hz octave band was not corrected.

Figure 21. Setup to redirect the acoustic emissions of a RSS.

The sound intensities of the large and small fan sources were measured in the US Lab Mockup as shown in Figs. 24 and 25. The floor of the mockup, made of one layer 0.5" MDF and one layer 0.75" plywood, provides sufficient transmission loss for shielding the measurement from background noise, particularly non-stationary background noise. A sheet of fiberglass backed Bisco® was placed under the measurement setup for further blocking fan emission from leaking through the bottom surface and reflecting the emission back to the measured surfaces. The Thinsulate curtains hung on the wall reduced acoustic reflection for the measurement. Figures 26 and 27 show sound intensity mappings of small/large fan outlets, i.e., the front surface of the grid system, for 2 kHz octave band. The intensities shown were interpolated from measurement by spline. Sound power estimated from interpolated intensity was compared to sound power estimated from non-interpolated intensity. The difference was found to be insignificant (smaller than 0.1 dB).

D. Model Validation for CM Mockup with Thinsulate, No ECLSS Wall, Excitation by Fan Source

The small fan was placed on the mockup deck in two orientations as shown in Figs. 28 and 29. Similarly, the large fan was placed on the mockup deck. The mockup model was validated based on SPL prediction accuracy over octave bands by comparing with measured SPL averaged across the two source orientations and the same ten microphones as used for the bare CM mockup. The prediction of the model matches well with the average of measured SPLs for excitation by small fan and large fan cases as depicted in Figs. 30 and 31. The three models of cavity absorption appear to make no significant difference in SPL prediction. Particularly, no correction for air absorption would be used for later mockup models with the ECLSS wall installed. Further reduction in air absorption is expected due to reduction in mean free distance between reflections.

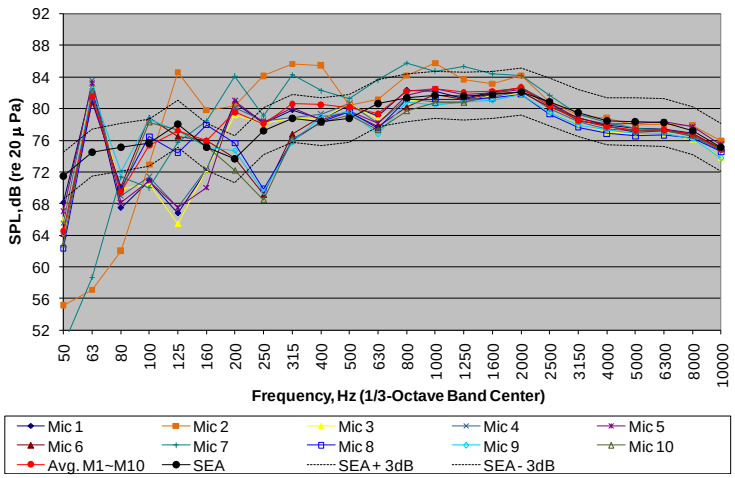

Figure 22. SEA prediction vs. measured SPL distribution in bare Orion CM Mockup, excitation by single RSS with restricted directivity and located at deck center.

E. Model of Bare CM Mockup, Bare ECLSS Wall with Open Gaps

Figures 32 and 33 show the ECLSS wall installed in the mockup with associated supporting beams and closeout panels. The mockup SEA model consists of:

- 4 SEA cavities, one for the cabin, the remaining three for the ECLSS bay, as shown in Fig. 34.
- 59 SEA plates for ECLSS wall, mockup wall/ceiling/floor, and ECLSS bay closeout panels, as shown in Fig. 35.
- 14 SEA beams for the 2-by-4 and 1-by-4 wooden beams supporting the ECLSS wall and closeout panels, as shown in Fig. 36.

- 31 manual area junctions for facilitating energy exchange among the acoustic cavities and surrounding plates without unnecessary division of the plates.
- 24 manual point junctions for connecting ECLSS wall supporting beams to mockup floor/ceiling and ECLSS wall.

The cavity absorption of the mockup was calculated from measured $\overline{T}_{60}$ using the Sabine equation. Again, the reverberation measurement was performed using the interrupted method and the B&K dodecahedron speaker. In addition to the ten microphones used before, three more microphones were used: one in starboard side ECLSS bay, the second one in center ECLSS bay, and the third one in port side ECLSS bay.

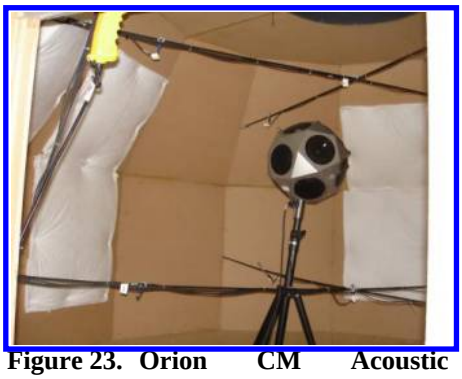

Figure 23. Orion CM Acoustic Mockup with 2 layers of Thinsulate and B&K dodecahedron speaker.

Gap models were constructed on SEA area junctions, which can be either a cavity-cavity connection or a cavity-plate-cavity connection. Energy exchange can go through one or several of the following parallel paths:[5]

- Resonant path for a cavity-cavity and cavity-plate-cavity connection.
- Nonresonant path for mass law transmission via a cavity-plate-cavity connection only. Nonresonant path is not available for a cavity-cavity connection, i.e., no mass law transmission.
- Leak/Flanking path for specifying a slit or rectangular leak on a cavity-cavity and cavity-plate-cavity connection.
- TL path for specifying a TL spectrum for a cavity-cavity and cavity-plate-cavity connection. This path was disabled and not used because the TL spectra of the gaps were not measured.

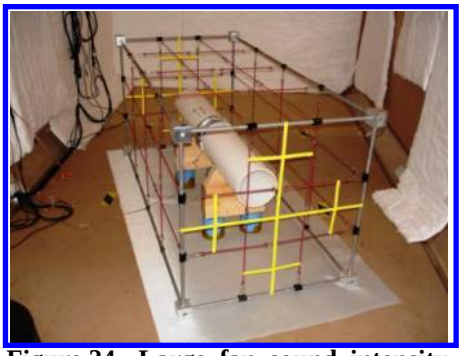

Figure 24. Large fan sound intensity measurement, fan exhaust to the back.

The locations of gap models inside the mockup system model are shown in Fig. 37. Several types of gap models were investigated:

1) Gap modeled as a simple opening on a cabin-ECLSS bay area junction with resonant path enabled. The resonant path couples both cavities directly. Leak/Flanking and TL paths were disabled. Both 15-gap and 5-gap models were used in the mockup model. The gaps in the same plane in a 15-gap model were merged to form a 5-gap model.
2) Gap modeled as a slit leak on a cabin-ECLSS bay area junction with resonant and TL paths disabled. Therefore, energy exchange between the two cavities is routed through the slit. Slit leak was used in both 15-gap and 5-gap models.
3) Gap modeled as a rectangular leak on a cabin-ECLSS bay area junction with resonant and TL paths disabled. Rectangular leak was used in both 15-gap and 5-gap models.
4) Gap modeled as a slit on the flanking path of a cabin-ECLSS wall-ECLSS bay area junction with TL path disabled. The resonant path accounts for the resonant transmission between the resonant modes of the cabin, the ECLSS wall, and the ECLSS bay. The nonresonant path accounts for the mass law transmission between the two cavities through the nonresonant modes of the ECLSS wall. This type of model has 9 gaps, each along the edge of one of the ECLSS wall panels.
5) Gap modeled as a rectangular leak on the flanking path of a cabin-ECLSS wall-ECLSS bay area junction with TL path disabled. Again, this type of model has 9 gaps.

Figure 25. Small fan sound intensity measurement, fan exhaust to the back.

F. Model Validation for Bare CM Mockup, Bare ECLSS Wall with Open Gaps

The mockup model was validated by placing sound source(s) in the ECLSS bay, which houses most of the noise sources in real Orion CM. The following three cases were performed:

1) Excitation by two RSSs: one in starboard side ECLSS bay, and the other in port side ECLSS bay, as shown in Fig. 38.
2) Excitation by large fan in center ECLSS bay, as shown in Fig. 39.
3) Excitation by small fan in center ECLSS bay.

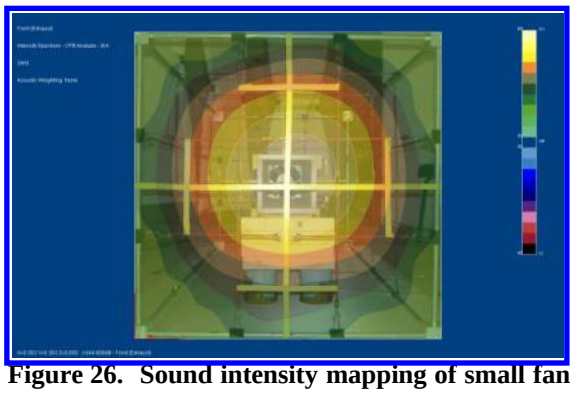

Figure 26. Sound intensity mapping of small fan outlet (front), 2 kHz octave band.

Comparing the various gap models on predicting cabin SPLs under the excitation by two RSSs indicates that

1) Slit leak generates higher cabin SPL than simple opening at most of the frequency range.
2) Rectangular leak generates slightly lower cabin SPL than simple opening at low and mid frequencies and virtually the same SPL at high frequencies.
3) 15-gap model produces similar cabin SPL as corresponding 5-gap model.
4) 5-gap model produces virtually the same cabin SPL as corresponding 9-gap model, which was defined on the flanking paths of cabin-ECLSS wall-ECLSS bay area junctions.

Figures 40 and 41 show the above observations. Additional validations of these models under large and small fan excitation show similar trend as RSS excitation. Based on the above observation, 9-gap models were not used for further study.

G. Model of Bare CM Mockup, Bare ECLSS Wall with Sealed Gaps

Fiberglass backed Bisco with density 0.246 lb/ft^2 was used for sealing the gaps between the ECLSS wall and the mockup wall as shown in Fig. 42.

No reverberation time test was performed for this mockup configuration. Absorption coefficients for the cabin and the ECLSS bay were adopted from the open-gap mockup model.

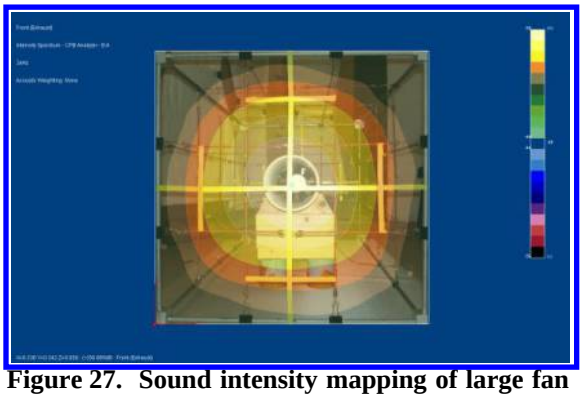

Figure 27. Sound intensity mapping of large fan outlet (front), 2 kHz octave band.

Three models of a sealed gap were investigated:

1) Sealed gap modeled as a one layer of Septum on the cabin face that is collocated with the gap as shown in Fig. 43. Septum represents a layer of SEA NCT with negligible stiffness possessing attributes of mass per unit area and thickness. Septum exhibits pure mass law transmission in mid and high frequencies as shown in Fig. 45. The resonant path of the gap area junction was enabled. Under this construction, the Septum was in **series** with the gap. Leak/Flanking and TL paths were disabled. The nonresonant path was not available due to the cavity-cavity area junction involved here. This type of construction was used in both 15-gap and 5-gap models.
2) Sealed gap with leak. This model is similar to the model in 1), but the leak/flanking path was enabled with a rectangular leak. The width and depth of the leak was close to the thickness of the Bisco. The TL path was still disabled. Under this construction, the leak was in **parallel** with the Septum-gap path as shown in Fig.44. This type of construction was used in both 15-gap and 5-gap models.
3) Perfectly sealed gap by disabling a gap area junction. The four parallel transmission paths through the area junction, as described in section E, were blocked automatically regardless their original setup. This type of construction was used in 5-gap models only. A 15-gap model will render the same prediction as a 5-gap model because the same total acoustic coupling areas are blocked for both models.

SEA VTL analysis was performed on standalone gap models, i.e., gap models were not included in a mockup system model. The resulting TL curves of these gap models are shown in Fig. 45, which indicates that

1) Sealed gap modeled as a one layer of Septum without a leak shows a pure mass law blocking effect. The TL curve of the gap has a slope of 6 dB/octave in mid and high frequencies.

2) The effect of introducing a small leak to a sealed gap depresses the TL of the gap only in mid and high frequencies. The TL curve saturates at high frequencies. The larger the gap size, the lower the maximum the TL curve reaches and the lower the frequency the TL curve starts leveling off. Also, the maximum TL is very sensitive to the gap size.

H. Model Validation for Bare CM Mockup, Bare ECLSS Wall with Sealed Gaps

The mockup model was validated similarly as the mockup model with open gaps, and the same set of microphones were used. Validation with excitation by two RSSs indicates that

1) Sealed gap modeled as a one layer of Septum tends to underestimate habitable volume SPL at **high** frequencies. Introducing a small leak improves the estimation accuracy significantly as shown in Fig. 46. The size of the leak is on the order of Bisco thickness. The fiberglass backed Bisco was placed over the gaps and attached to the ECLSS wall panel and mockup wall by Kapton tape. Leaking was expected after tearing down and reapplying the sealing repeatedly for multiple test configurations. The most significant discrepancy between the measurement and the predictions of models without leaks is at high frequencies, which is typically caused by a leak in the measurement setup.
2) Again, 15-gap and 5-gap models generate similar cabin SPL.
3) Perfectly sealed gap model produces similar cabin SPL as models with 1-layer of Septum and no leak.
4) Additional improvement on estimation accuracy, particularly in mid frequencies, can be achieved by changing the DLFs of ECLSS wall and ECLSS bay closeout panels as shown in Fig. 46. DLF is the biggest unknown parameter in modeling these panels. There will be more discussion of this in later section.

Figures 47 and 48 show that validations of these models under large and small fan excitation exhibit similar trend as RSS excitations.

The effect of gap sealing was studied by calculating the IL before/after sealing the gaps. IL was computed by subtracting the cabin SPL (dB) after sealing the gaps from the cabin SPL (dB) before sealing the gaps. The predicted IL was calculated from cabin SPLs using various mockup models, while the measured IL was calculated from average of measured cabin SPLs at the ten microphones. The results of excitation by two RSSs were used for the calculation because the flat spectrum of RSS excitation provided better signal-to-noise ratio. Figure 49 shows that a small leak improves IL estimation of gap sealing at high frequencies and that the DLF changes to ECLSS wall/closeout panels further improves the IL estimation in mid to high frequencies. There will be more discussions on DLF changes in Section J.

Based on the above observations, 15-gap models were not used in the following studies.

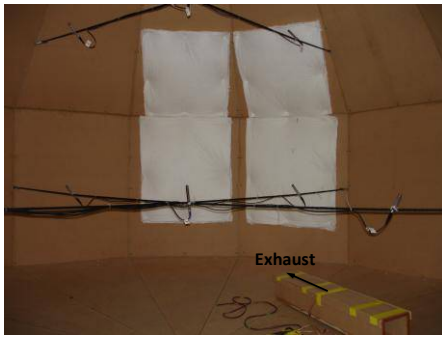

Figure 28. Small fan in Orion CM Acoustic Mockup, orientation 1.

Figure 29. Small fan in Orion CM Acoustic Mockup, orientation 2.

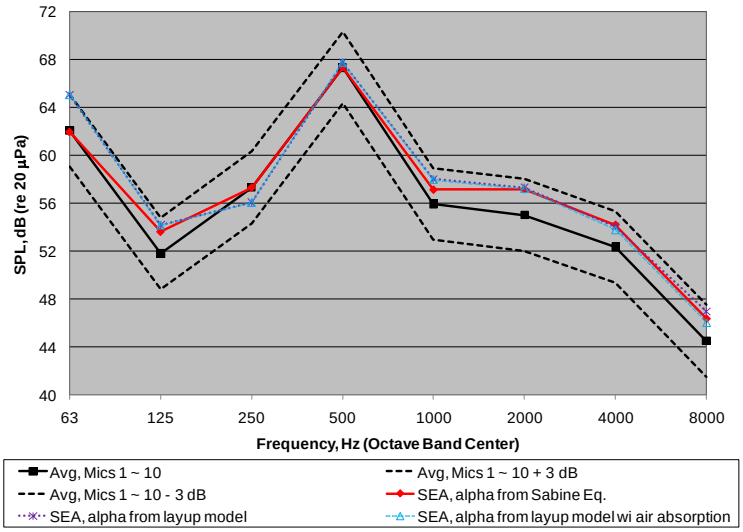

Figure 30. SEA prediction vs. average of measured SPLs in Orion CM Acoustic Mockup covered by 2 layers of Thinsulate, excitation by small fan, absorption from various models.

I. Model of Bare CM Mockup, ECLSS Wall with Sealed Gaps, One Layer of Thinsulate Attached to ECLSS Wall

Two cases of Thinsulate attachment were investigated. Figure 50 shows the first case where all of the Thinsulate was attached to the cabin side of the ECLSS wall. Figure 51 shows the second case where part of the Thinsulate was attached to the cabin side of the ECLSS wall (on 4 panels) and remaining part of the Thinsulate was attached to the ECLSS bay side of the ECLSS wall (on 3 panels).

Reverberation time measurements were performed for both the cabin and the ECLSS bay. Again, the B&K dodecahedral speaker was placed at 6 locations in the cabin for measuring the T_{60} of the cabin. But, the dodecahedral speaker was not used to measure the T_{60} of the ECLSS bay because the speaker size was relatively large compared to the bay. This would have brought the speaker too close to some of the microphones. Therefore, a Boston Acoustics VS260 bookshelf speaker was used and placed at 4 locations in the bay.

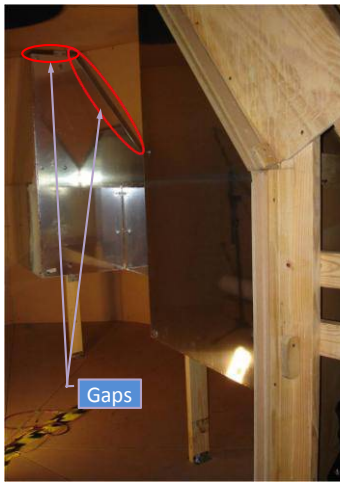

Figure 32. ECLSS wall in Orion CM Acoustic Mockup with open gap.

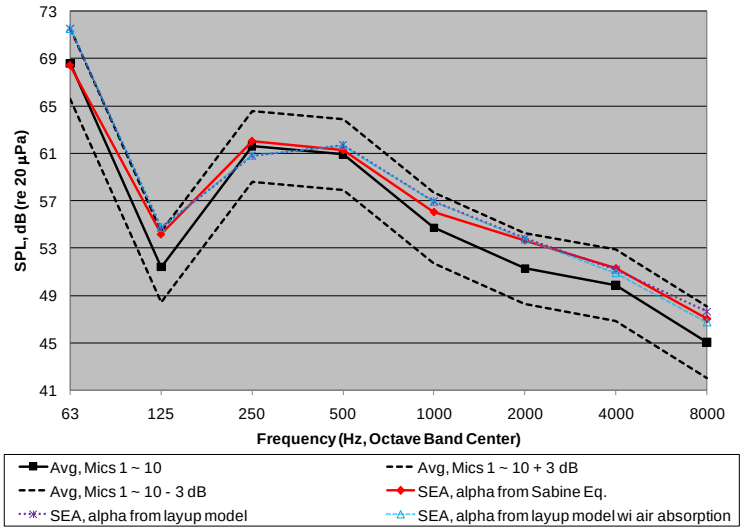

Figure 31. SEA prediction vs. average of measured SPLs in Orion CM Acoustic Mockup covered by 2 layers of Thinsulate, excitation by large fan, absorption from various models.

The mockup model contained 5 sealed gaps with rectangular leaks as described in Section G. Area-averaged absorption spectra from various combinations of Sabine equation with measured T_{60}, Thinsulate layup model based on past impedance tube testing, and absorption of MDF based on impedance tube testing were used to specify the absorption spectra of the cabin and the ECLSS bay.

Thinsulate absorption in the cabin and in the ECLSS bay was estimated from the Thinsulate layup model and measured T_{60}. The thickness of the Thinsulate patches deployed in the mockup was not constant due to gravitation and from wrapping around ECLSS wall supporting beams. The average thickness was estimated to be close to 56 mm. SEA cavity absorption analysis of the cabin and the ECLSS bay with the Thinsulate layup model on the ECLSS wall for Cases 1 and 2 was performed. The resulting cavity absorption was considered to be contributed from Thinsulate covered areas and non-Thinsulate areas, i.e., bare ECLSS wall, bare mockup wall, docking tunnel, etc. This can be expressed as follows.

$$\begin{bmatrix} S_{t_1} & S_{b_1} \\ S_{t_2} & S_{b_2} \end{bmatrix} \begin{Bmatrix} \alpha_t \\ \alpha_b \end{Bmatrix} = \begin{Bmatrix} \alpha_1 \\ \alpha_2 \end{Bmatrix} S \tag{4}$$

where

α_t a is the absorption of Thinsulate.

α_b a is the absorption of non-Thinsulate area.

α_1 and α_2 are the absorption of the cabin (or the ECLSS bay) for Case 1 and 2, respectively.

S_{t_1} and S_{t_2} are Thinsulate covered areas in the cabin (or the ECLSS bay) for Case 1 and 2, respectively.

S_{b_1} and S_{b_2} are non-Thinsulate areas in the cabin (or the ECLSS bay) for Case 1 and 2, respectively.

S is total surface area of the cabin (or the ECLSS bay). Note: $S = S_{t_1} + S_{b_1} = S_{t_2} + S_{b_2}$.

Eq. (4) can be solved for α_t (and α_b) for all the frequency bands. It was found that α_t saturates above certain frequency. The thicker the Thinsulate layup, the lower the frequency α_t saturates. However, the levels of absorption after saturation were similar for various thicknesses. Instead of using SEA cavity absorption analysis, an alternative method was to use Eq. (4) to solve for α_t from T_{60}-derived cavity absorption. It was found that the above two methods did not render similar values for α_t .The discrepancy may be attributed to the fact that the cabin and ECLSS bay were not isolated from each other during T_{60} tests. In other words, the absorption in one cavity might affect the T_{60} of the other cavity.

In order to estimate the MDF absorption in the cabin and the ECLSS bay, large and small samples of 2-layered MDF were tested in a B&K 4206T impedance tube. The measured impedance ratio was used to estimate random incidence absorption coefficients of both large and small samples based on a formula in ISO 10534-2.[2] These random incidence absorption coefficients were then combined using the following B&K provided formula.

$$\alpha(f) = A \times \alpha_{large}(f) + (1 - A) \times \alpha_{small}(f) \tag{5}$$

where

$$A = \begin{cases} 1, & f < 500 \\ 1 - [(f - 500)/1600 - 500], & 500 \le f \le 1{,}600 \\ 0, & f > 1{,}600 \end{cases}$$

The combined absorption spectrum follows the large sample absorption for frequencies less than 500 Hz, the small sample absorption for frequencies above 1.6 kHz, and a linear interpolation of large and small sample absorption for the frequency range from 500 Hz to 1.6 kHz. The resulting narrowband absorption spectrum was then converted to 1/3-octaveband spectrum. An "User Defined Treatment," with reference to the combined absorption spectrum, was then attached to the faces of the cabin and the ECLSS bay cavities where MDF wall panels were located.

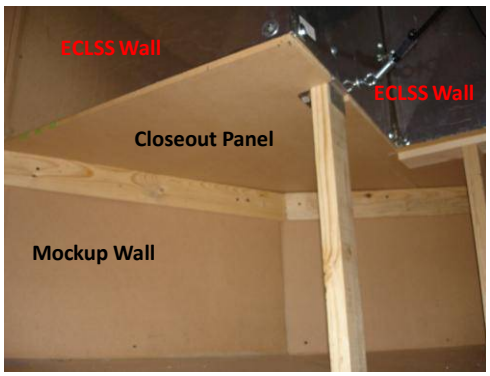

Figure 33. ECLSS wall supporting beams and closeout panels.

Several cavity absorption models for the cabin and the ECLSS bay were investigated:

1) Absorption spectra derived from the Sabine equation with measured T_{60} of the sealed-gap mockup. These spectra were used for Cases 1 and 2.
2) Absorption spectra derived from the Sabine equation with measured T_{60} of the open-gap mockup for the ECLSS bay under Case 1. These spectra were used for Case 1 only.
3) Absorption spectra derived from area-average of α_t from T_{60} tests of the sealed-gap mockup with Thinsulate attachment Cases 1 & 2 and α_b from T_{60} test of the open-gap mockup. These spectra were used for Cases 1 and 2. The area-average spectra were calculated as follows.

$$\begin{aligned} \alpha^c &= \left[S_t^c \alpha_t + \left(S^c - S_t^c\right)\alpha_b\right] / S^c \\ \alpha^e &= \left[S_t^e \alpha_t + \left(S^e - S_t^e\right)\alpha_b\right] / S^e \end{aligned} \tag{6}$$

where superscripts "c" and "e" denotes the cabin and the ECLSS bay, respectively. The subscripts are defined similarly as in Eq. (4). Note: $S_t^c = S_{ECLSS\_wall}$ and $S_t^e = 0$, for Case 1.

4) Absorption spectra derived from SEA cavity absorption analysis with a 44 mm Thinsulate layup on the ECLSS wall and random incidence MDF absorption on the mockup wall for Cases 1 and 2. These spectra were used for Cases 1 and 2.
5) Absorption spectra derived from SEA cavity absorption analysis with a 56 mm Thinsulate layup on the ECLSS wall and random incidence MDF absorption on the mockup wall for Cases 1 and 2. These spectra were used for Cases 1 and 2.

Comparing cavity absorption of the above models indicates that

1) An increase in thickness of the Thinsulate layup (from 44 mm to 56 mm) yields an increase in cabin absorption below 800 Hz as shown in Fig. 52. This also occurs for ECLSS bay absorption for Case 2.
2) An increase in thickness of the Thinsulate layup has no effect on ECLSS bay absorption under Case 1 as shown in Fig. 53. Similarly, ECLSS bay absorption based on the model in 2) is the same as the absorption based on the model in 3), as shown in Fig. 54. This is because ECLSS bay has no Thinsulate under Case 1.
3) Cavity absorption predicted by the two SEA models in 4) and 5) (the cyan and yellow curves) is higher compared to the absorption predicted by the remaining models at high and/or mid frequencies. This is shown in Figs. 52 and 53. The remaining models use T_{60}-derived absorptions, which could be affected by absorption coupling between the cabin and the ECLSS bay.
4) Under Case 1, the ECLSS bay absorption based on the model in 1) (the blue curve) is higher than the absorption based on the model in 2) (the purple curve, which is overlaid by the orange curve), as shown in Fig. 53. This clearly indicates that there is absorption coupling problem. If there is no absorption coupling, we should have the same absorption because the ECLSS bay is **bare** under Case 1. Note that the absorption model in 1) was derived from T_{60} tests with Thinsulate attached to the ECLSS wall on the cabin side while the absorption model in 2) was derived from T_{60} tests without Thinsulate present. The absorption of the Thinsulate on the cabin side of the ECLSS wall must contribute to the absorption of the **bare** ECLSS wall under Case 1.

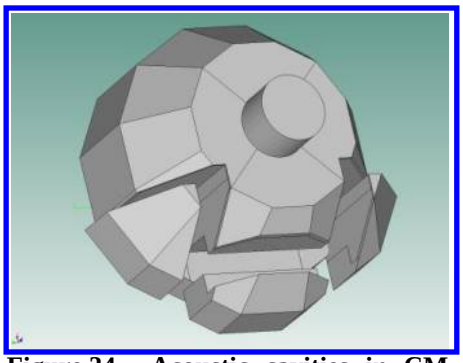

Figure 34. Acoustic cavities in CM Mockup model, exploded view.

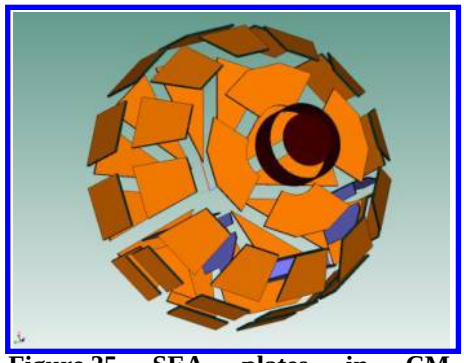

Figure 35. SEA plates in CM Mockup model, exploded view.

J. Model Validation for Bare CM Mockup, ECLSS Wall with Sealed Gaps, One Layer of Thinsulate Attached to ECLSS Wall

The mockup model was validated similarly as the mockup model with open gaps except that no large fan was used. The same set of microphones were used. Validation with excitation by two RSSs indicates that models with cavity absorption derived from T_{60} tests tend to overestimate habitable volume SPL, while models with cavity absorption derived from layup models and MDF random incidence absorption have better estimation of habitable volume SPL, as shown in Fig. 54. This is consistent with the observation that the cavity absorption in the latter tends to be higher.

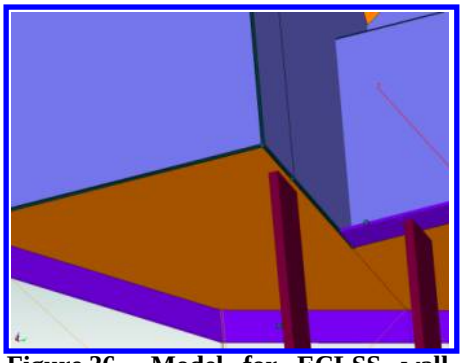

Figure 36. Model for ECLSS wall supporting beams and closeout panels.

The SPL prediction accuracy as shown in Fig. 54 can be further improved, particularly the overestimation for the frequency range from 630 Hz to 2.5 kHz. Increasing the thickness of the Thinsulate layup was first considered and ruled out as a cause because it was only effective below 800 Hz as described above. The next potential cause investigated was the resonant transmission of ECLSS wall and ECLSS bay closeout panels. Resonant transmission is caused by the matching of acoustic and structural wavelength, i.e., the phenomenon of "coincidence." The frequency of coincidence is called the critical frequency. Critical frequency can be detected by the crossing of the curves of acoustic and structural wave number, which is inversely proportional to wavelength.

It was found that the critical frequencies for the ECLSS wall and ECLSS bay closeout panels are located in the frequency bands of 630 Hz and 2 kHz, respectively. Investigation of the power inputs to the habitable volume indicated that inputs from panel resonant transmissions start dominating inputs from non-resonant (mass law) transmissions for frequency above 800 Hz. This is consistent with the fact that "coincidence" occurs only at and above, not below, the critical frequency. Unlike non-resonant transmission, resonant transmission can be controlled by damping. It has been recognized that the DLF of a structural panel is important to predictive SEA models, but is difficult to model. An experimental SEA technique called PIM was developed to measure damping and other parameters for fine tuning predictive SEA models[6,7]. Without measured DLF, the value is set at 1% as default by VA One. We plan to implement DLF measurement in the near future. Adjustments of DLFs to the ECLSS wall and ECLSS bay closeout panels were performed to investigate if the overestimation in 630 ~ 2,500 Hz could be improved. Only the DLF of flexural wavefield was changed because this is the only wavefield that can couple to the sound field of the cabin. The best fitting configuration for DLF was found to be: 1% across most of the frequency range except twin maximums of 7.5% at 630 Hz and 1.6 kHz for the ECLSS wall panels, and 5% across the whole frequency range for the closeout panels. Fig. 55 indicates that these adjustments were very effective.

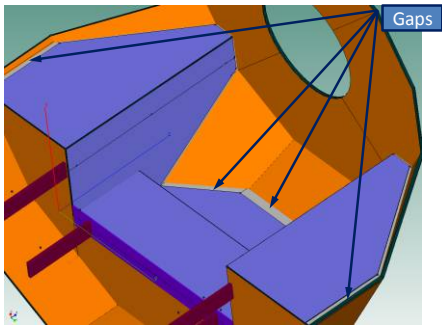

Figure 37. Gaps in CM Acoustic Mockup model.

Figure 38. RSSs at port side ECLSS bay and starboard side ECLSS bay.

Figure 39. Large Fan at center ECLSS bay.

It was found by both measured and predicted cabin SPL, as shown in Fig. 56, that deploying part of the available Thinsulate treatments inside the ECLSS bay, i.e., Case 2, is more effective in reducing the cabin SPL than deploying all the treatments in the cabin, i.e., Case 1. The result can be illustrated in terms of Thinsulate contribution to the area-averaged cavity absorption. For the same Thinsulate covered area S_t, the absorption contribution to the cabin is $S_t\alpha_t/S^c$, while the absorption contribution to the ECLSS bay is $S_t\alpha_t/S^e$. Since the habitable volume has larger total surface area than the ECLSS bay, i.e., $S^c > S^e$, the absorption contribution to the ECLSS bay is larger. Therefore, it is more efficient to absorb the noise in the ECLSS bay before it escapes to the cabin, where a larger treatment area is required to absorb the escaped noise. This result is useful for noise radiated directly into the ECLSS bay. For noise that is radiated directly into the cabin (e.g. a ventilation duct connected directly to the cabin, or a noise source inside the cabin), the absorption treatment in the ECLSS bay will not be effective.

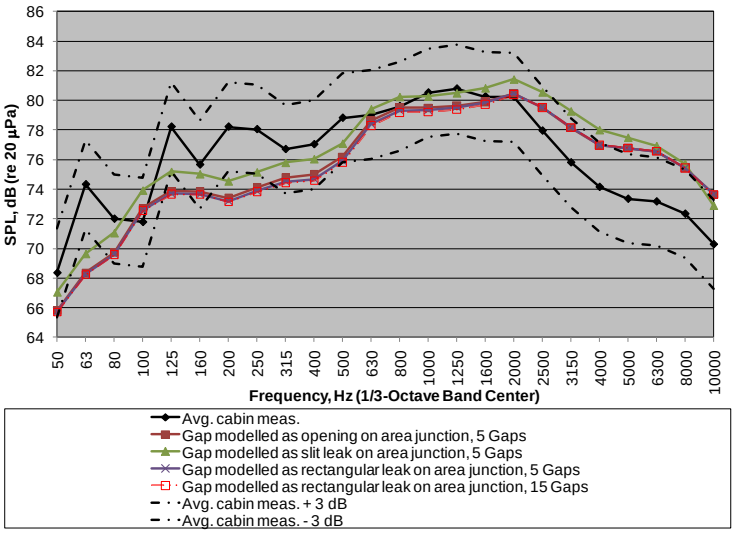

Figure 40. SEA prediction by various 5-gap and 15-gap models vs. average of measured SPLs in the cabin of CM Mockup with open gap, excitation by two RSSs.

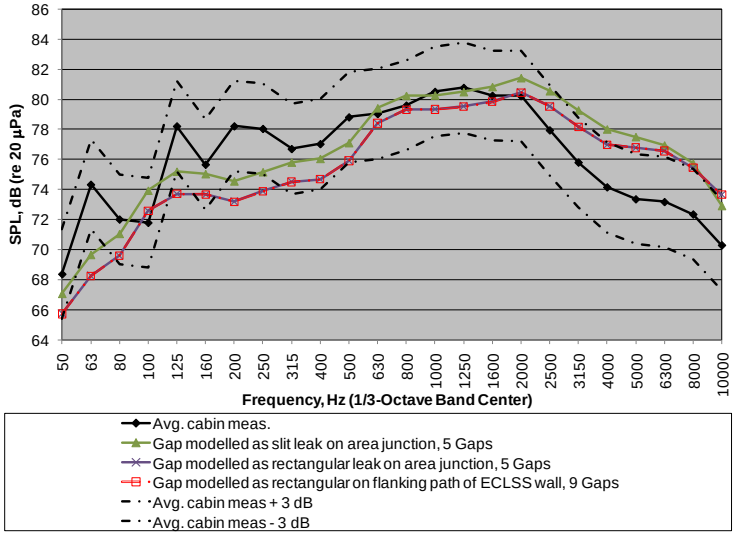

Figure 41. SEA prediction by various 5-gap and 9-gap models vs. average of measured SPLs in the cabin of CM Mockup with open gap, excitation by two RSSs.

Figure 42. ECLSS wall in Orion CM Acoustic Mockup with gap sealed by fiberglass backed Bisco.

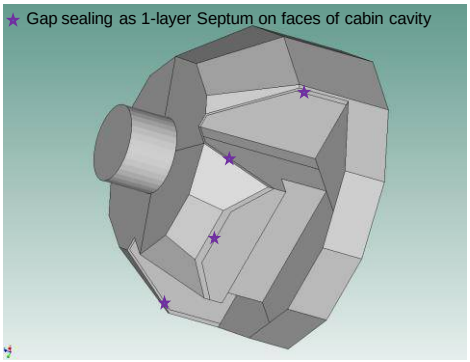

Figure 43. Gap sealing model.

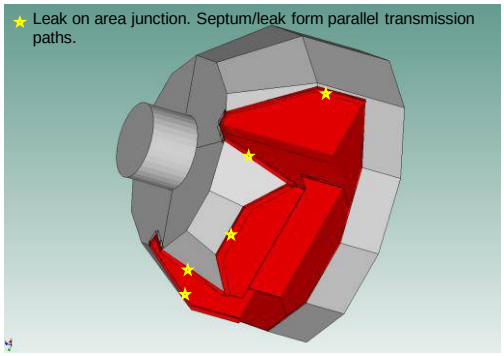

Figure 44. Leaky gap sealing model.

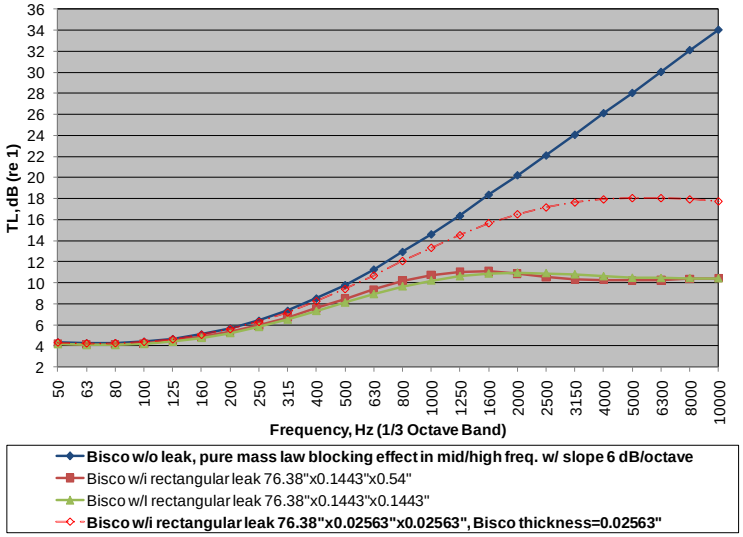

Figure 45. TLs of various standalone Bisco sealed gap models, with and without leak, in length x width x height.

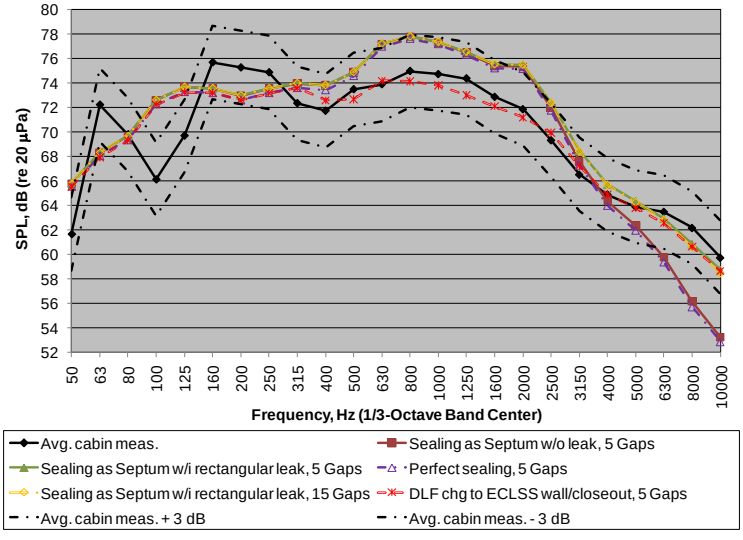

Figure 46. SEA prediction by various 5-gap and 15-gap models vs. average of measured SPLs in the cabin of CM Mockup with sealed gap, excitation by two RSSs.

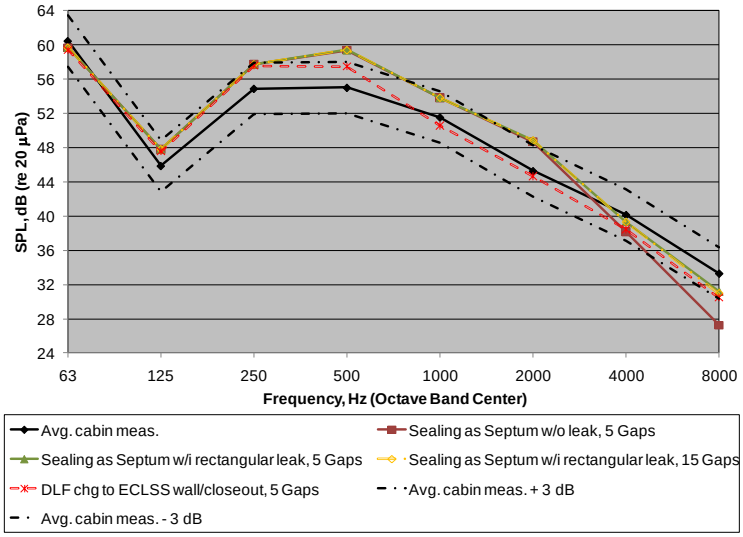

Figure 47. SEA prediction by various 5-gap and 15-gap models vs. average of measured SPLs in the cabin of CM Mockup with sealed gap, excitation by large fan.

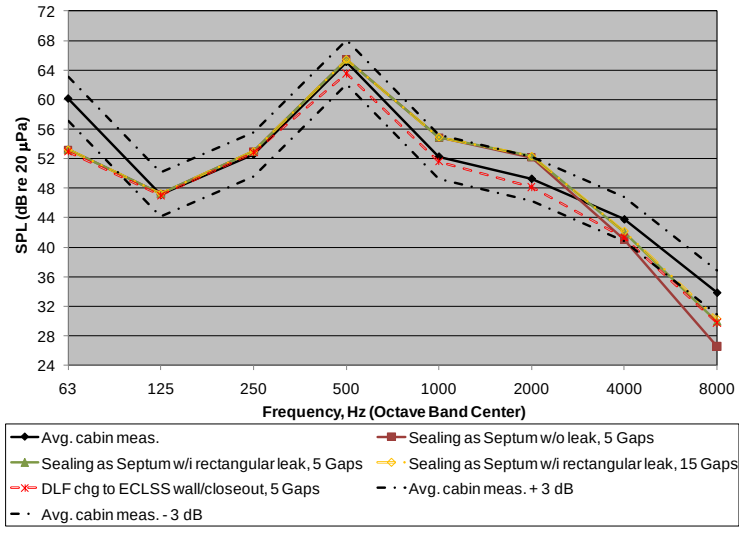

Figure 48. SEA prediction by various 5-gap and 15-gap models vs. average of measured SPLs in the cabin of CM Mockup with sealed gap, excitation by small fan.

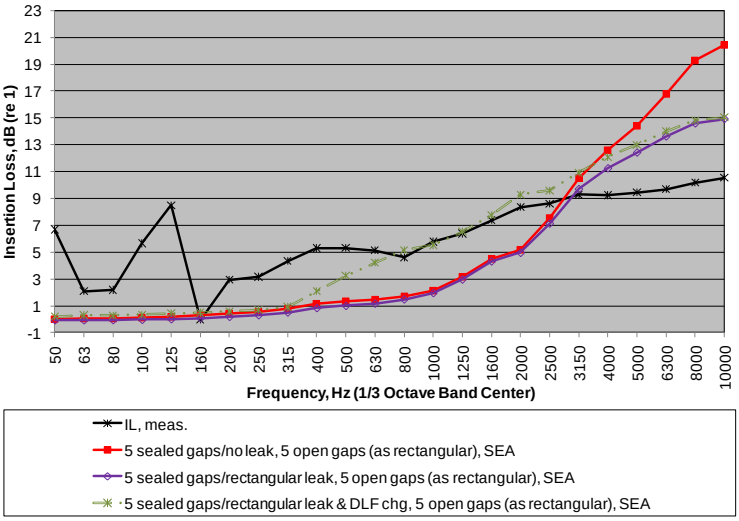

Figure 49. IL of gap sealing, SEA prediction vs. measurement

Figure 50. Thinsulate attachment Case 1: all attached to cabin side of ECLSS wall.

Figure 51. Thinsulate attachment Case 2: some attached to cabin side of ECLSS wall, the remaining attached to ECLSS bay side of ECLSS wall.

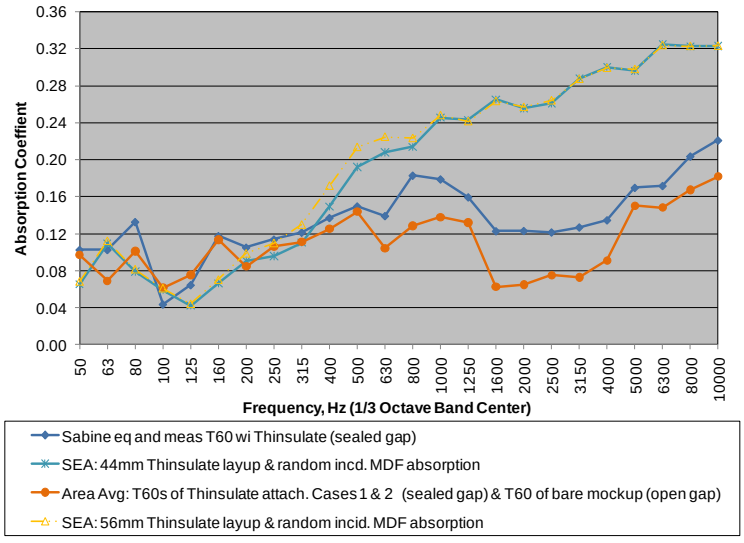

Figure 52. Cabin cavity absorption for Thinsulate covered ECLSS wall with sealed gaps, Case 1

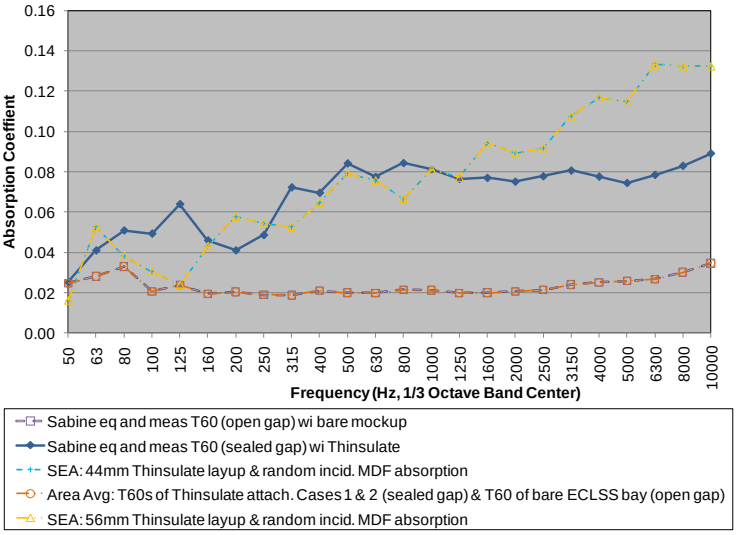

Figure 53. ECLSS bay cavity absorption for Thinsulate covered ECLSS wall with sealed gaps, Case 1

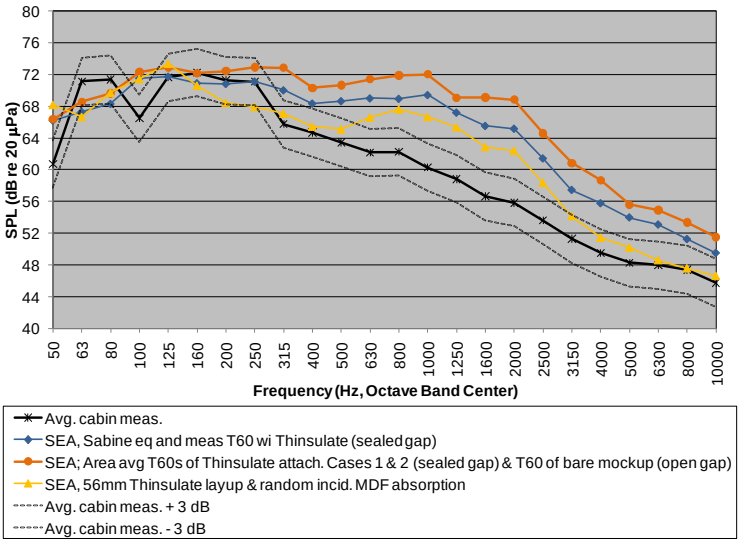

Figure 54. SEA prediction vs. average of measured SPLs in the cabin of CM Mockup with Thinsulate covered ECLSS wall and sealed gap, Case 2, excitation by two RSSs.

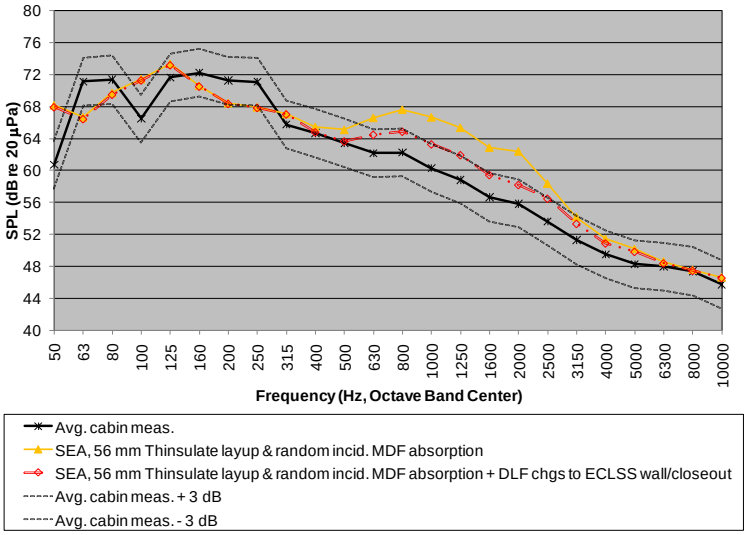

Figure 55. Effect of DLF changes on predicting cabin SPL of CM Mockup with Thinsulate covered ECLSS wall and sealed gap, Case 2, excitation by two RSSs.

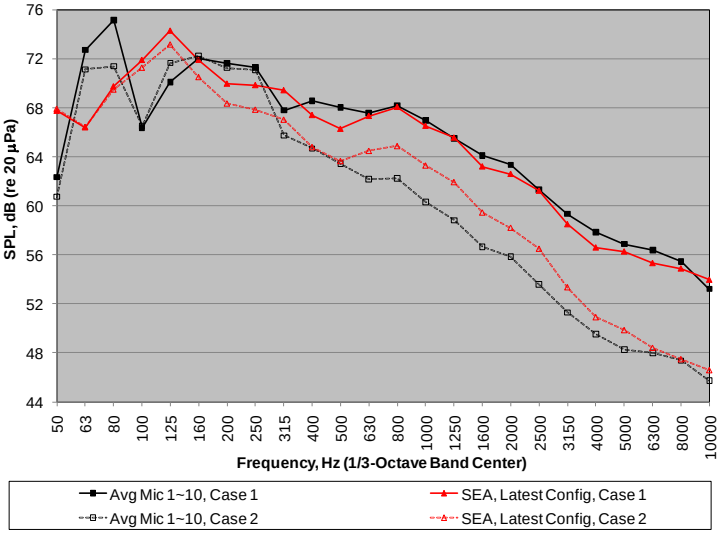

Figure 56. Thinsulate attachment Case 1 vs. Case 2 on predicted and measured cabin SPL, excitation by two RSSs.

IV. Conclusion and Future Work

This paper demonstrates the development of spacecraft cabin acoustic models and a model validation technique using acoustic mockups with incrementally increasing fidelity. The modeling of the ISS US Lab mockup with a simple rectangular-shaped interior was first performed. Three mockup interior reverberant environments were modeled and validated successfully using single and dual airborne sound sources, i.e., RSSs. Two methods were developed to model the mockup interior absorption: one was based on the measurement of mockup interior reverberation time T_{60}; the other was based on impedance tube measurement of sound absorption material used to cover the interior surfaces of the mockup. The effect of source location on the accuracy of the model predictions under a highly absorptive mockup interior was observed. Furthermore, it was demonstrated that appropriately subdivided SEA cavities can model the SPL distribution in a large mockup with a highly absorptive interior.

The Orion CM mockup with a more complex geometrical shape was then modeled. In addition to RSS(s), ventilation fans with sound power levels unknown beforehand were used for the modeling/validation process. Sound power levels of the ventilation fans were estimated from sound intensity measurements. The fidelity of the mockup and the model were increased from an empty interior in the beginning to include an ECLSS wall and ECLSS bay with open/sealed gaps and two configurations of attached Thinsulate to the surfaces of the ECLSS wall panels. Results from this investigation prompted and supported the development of similar system level noise treatments for the actual Orion vehicle. Also, lessons were learned regarding the problem of absorption coupling between cavities and the problem of DLF sensitivity on modeling structure-borne noise. Moreover, it was found by both modeling and measurement that deploying part of available absorption material in the ECLSS bay was more effective in reducing cabin SPL due to a noise source in the ECLSS bay than deploying all of the absorption material in the cabin.

Subsequent to the work described in this paper, Aluminum sheets were attached to the interior surfaces of the Orion CM mockup wall for increasing the interior reverberation time to a more realistic level because the MDF wall is more absorptive compared to typical metallic surfaces of a spacecraft pressure vessel. Validation of the mockup model with the Aluminum interior will be performed in the near future. A new reverberation time testing procedure will be implemented to avoid the problem of absorption coupling. Also in 2012, the fidelity of the mockup will be further increased by including a secondary structure and storage lockers.

Acknowledgments

The authors would like to thank NASA Human Research Program (HRP), Constellation Program (CxP), and Crew Exploration Vehicle (CEV) Project Office for their supports. Also, the authors would like to thank Holly Smith, staff member of NASA JSC Acoustics Office, for her support in performing impedance tube tests of MDF samples and estimation of random incidence absorption of the samples.

References

[1]ISO 3382, "Acoustics – Measurement of the Reverberation Time of Rooms with Reference to Other Acoustical Parameters," 1997.

[2]ISO 10534-2, "Determination of Sound Absorption Coefficient and Impedance in Impedance Tubes – Part 2: Trasfer-Function Method," 1998.

[3]ASTM E1050, "Standard Test Method for Impedance and Absorption of Acoustical Materials Using A Tube, Two Microphones and A Digital Frequency Analysis System," 1998.

[4]Bies, D. A., Hansen, C. H., *Engineering Noise Control, Theory and Practice*, 2nd ed., E & FN Spon, New York, 1996, pp. 176, 236.

[5]VA One 2010, User's Guide, ESI Group, 2010.

[6]Hermans, L., ladevaia, M., "Guidelines on the Use of Experimental SEA for Modeling and Understanding Road Noise in Cars," *Proceedings of the 1999 Noise and Vibration Conference*, Traverse City, Michigan.

[7]Lalor, J. L., "Practical Considerations for the Measurement of Internal and Coupling Loss Factors on Complex Structures," Institute of Sound & Vibration Research, Rept. No. 182, Jun. 1990.

[8]VA One 2010 Foam Module, User's Guide, Theory & QA, ESI Group, 2010.